IN-PLANE BEHAVIOR OF A STONE MASONRY PIER: EXPERIMENTAL TEST, NUMERICAL SIMULATION AND RETROFITTING EFFICIENCY EVALUATION

A. A. Costa, B. Silva, A. Arêde & J. M. Guedes

Faculty of Engineering, Department of Civil Engineering, Porto, Portugal

A. Costa

University of Aveiro, Department of Civil Engineering, Aveiro, Portugal

SUMMARY

This work aims to presenting a laboratory test of an existing Azorean stone masonry pier, transported to the Laboratory for Earthquake and Structural Engineering (LESE, FEUP, Porto), exhibiting significant energy dissipation but small displacement capacity. A complete 3D non-linear numerical simulation of the experimental test was also performed for simulating the observed response and good results were obtained, encouraging the use of this methodology either for calibration of other simplified models or in future works. After the first test, the pier was retrofitted with a strategy as used after the 1998 Azores earthquake and subsequently tested in order to assess that retrofitting efficiency and to evaluate the seismic resistance improvement. Indeed the major objective of that technique was achieved because a homogeneous and monolithic behaviour was observed, improving especially the displacement capacity of the pier.

1. INTRODUCTION

The 1998 Azores earthquake has severely damaged 5000 buildings and destroyed 2100 in Faial Island, from a total amount of 12624 edifications (INE, 2002). The main cause of this destruction was essentially related to the seismic action characteristics (near fault and shallow crustal earthquake) and, last but not the least, to the Azorean construction type. Actually, most of the existing buildings in the archipelago are made of stone masonry, which is known to exhibit non-satisfactory behaviour under earthquake action.

Therefore, particular interest was put on the mechanical characterization of these constructions and, even more important, on the in-plane and out-of-plane behaviour assessment of such type of buildings.

Hence the present work seeks first for experimentally and numerically characterizing the behaviour of a traditional double leaf stone masonry pier and, second, for the efficiency assessment of a strengthening technique widely used during the reconstruction/retrofit/rehabilitation process of the Faial Island.

2. PIER CHARACTERISTICS AND EXPERIMENTAL TEST SETUP

2.1. Test specimen

The tested pier was extracted from a two storey house (Figure 1-a) located at Pedro Miguel parish, Horta council, Faial Island of the Azores Archipelago. The wall was located at the ground floor between two main doors of the house façade, as it is possible to observe in Figure 1-b.

a).  b). 

Figure 1: Original location of the wall: a). General view; b). detailed view

The specimen consists of a traditional double leaf stone masonry wall with poor cohesionless infill material and covered with cement mortar, as commonly found in most of the old constructions in the Archipelago,.

This wall was sea-transported from its original location to the Laboratory for Earthquake and Structural Engineering LESE) of the Faculty of Engineering of the University of Porto, after an initial preparation and packing procedure in order to ensure its integrity.

A reinforced concrete foundation was built in the laboratory and the wall was placed inside, over a sand layer in order to simulate adequately the *in-situ* restrain conditions.

A stiff concrete plate and steel metallic shapes were placed at the top of the wall to allow uniform distribution of the horizontal and vertical loads applied to the specimen during the test.

2.2. Experimental test setup

A cantilever test setup (fixed at the base and free at the top) was used to assess the in-plane behaviour (Figure 2). Two hydraulic jacks were installed on the top beam, reacting against two steel plates and connected to the foundation through hinged steel rods, in order to impose the vertical load supposed to act on the pier in the real building before the roof and floor collapse. A total force of 35 kN was applied, corresponding to the 1st floor wall and pavement and to the timber roof loads.

a).  b). 

Figure 2: Specimen visualization: a) under test; b) final cracking pattern

The applied load pattern consisted on an incremental cyclic load up to a maximum drift level of 0.85%. Indeed some further displacements could have been achieved but it may have led to partial collapse of the wall which was not desirable in order to proceed with a suitable retrofitting. The criterion to stop the test was also related to the achieved maximum strength decrease of 85% that may be considered a reasonable value.

In order to correctly monitor the wall response, several displacement transducers were adopted aiming at recording all possible movements, as shown in Figure 3.

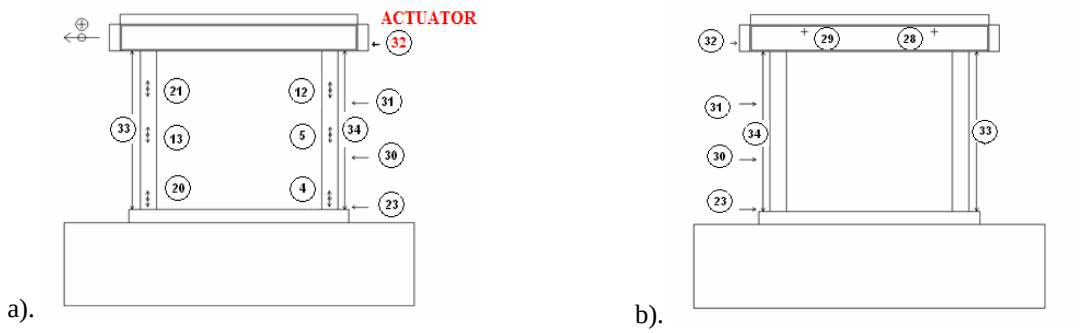

Figure 3: LVDT's positioning: (a) front view, (b) back view.

3. RESULTS INTERPRETATION

Several types of results were obtained from the experimental tests, from which the most important are herein presented in terms of both global and local behaviour.

3.1. Global behaviour

The global behaviour exhibited by the wall is presented in the form of hysteresis loops (force vs. displacement curve) as shown in Figure 4, that allows observing a global behaviour in sliding shear explained by the existing discontinuity surfaces in height.

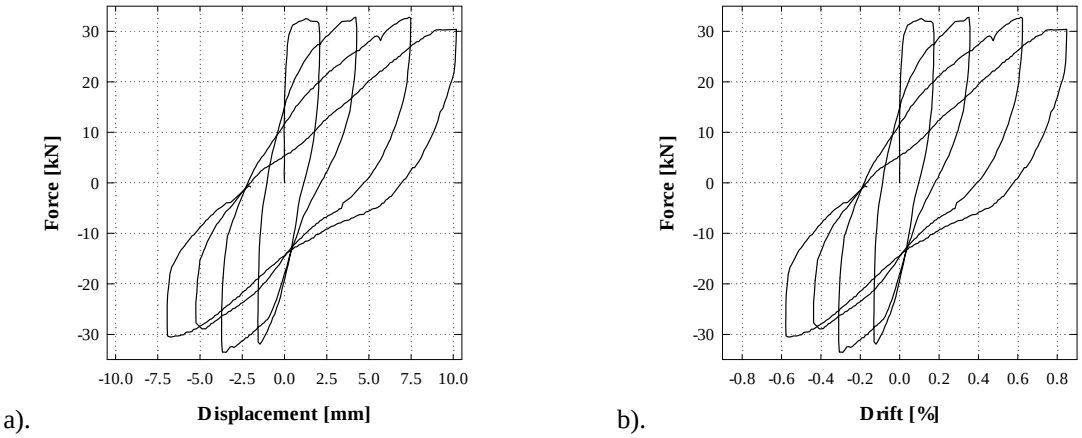

Figure 4: Force vs. :a) displacement; b) drift level

As evidenced by the force vs. displacement curve, the masonry wall exhibits a good energy dissipation capacity. Notice that for displacements imposed in the positive direction, the wall looses resistance in successive loading cycles for the same displacement level. In particular, from the 4 mm to the 6 mm loading cycle, there was a local strength drop of ~20% at 4 mm, which was recovered at the cycle end, i.e., for the 6 mm displacement. However, the last loading cycle shows that a non-recoverable strength loss occurred, since the curve seems incapable of reaching the previous cycle strength capacity.

The initial stiffness decay as obtained in the first branch of the graph may be due to destruction of connections at the joints levels that lead to progressive stiffness loss upon each consecutive displacement levels.

The displacement ductility capacity of this wall was considerably high, but if more cycles (3, for instance) were performed for the same displacement level, lower ductility could be expected.

3.2. Local behaviour

Despite the large amount of available information, the data herein presented refers to the lateral displacement along the wall height that is used for comparison with the numerical results considering the monitored points depicted in Figure 3.

Displacement time histories and in height profiles are included in Figure 5, from which it is possible to conclude that, despite an initial cohesion, the wall bed joints lost their integrity leading to sliding shear behaviour. This mechanism caused the upper part of the wall to slide over its middle part, as can be inferred from Figure 5 b), for time step N = 8000 and N = 9000.

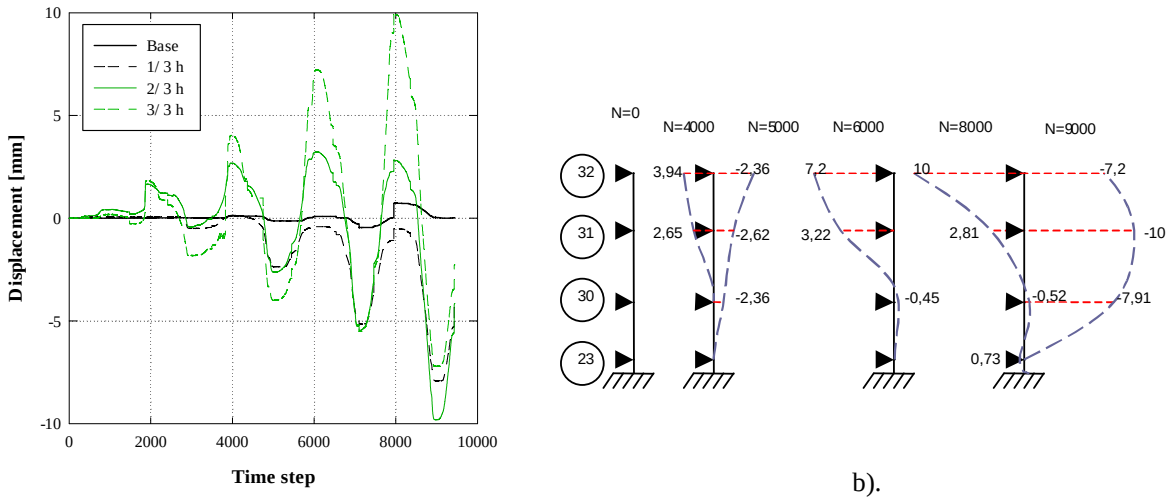

a). b).

Figure 5: Lateral displacement vs. time: a) evolution over time; b) deformed shape for different time steps (N)

4. NUMERICAL MODELLING

The numerical modelling approach used for the tested wall consisted on a full 3D discretization of the geometry and its representation with a discontinuous finite element model containing blocks, joint elements and infill. In addition, the top beam was also simulated as a stiff element in order to allow completely describing the performed experiment with all its real conditions during the test (axial load, displacement levels and monitored points). The finite element program used in this analysis was the program Visual Cast3m (CEA, 2003).

4.1. FE mesh and calibration

Figure 6 shows the complete geometry discretization of the tested wall, divided according to each type of elements, as well as the final full FEM mesh.

The compatibility between the numerical model and the real wall was calibrated resorting to modal analyses that allowed defining elastic characteristics of each component of the numerical model. Hence, both the blocks and the joints were calibrated starting with values found and used in previous works (Costa, 2002a), (Almeida, 2000) and (Costa, 2002b), while the infill properties were based on the values obtained through experimental tests performed by (Costa, 2002a). The adopted values as presented in Table 1, led to the numerically obtained vibration mode shapes shown in Figure 7 in correspondence with frequency values listed in Table 2 where experimentally obtained ones are also included for comparison purposes.

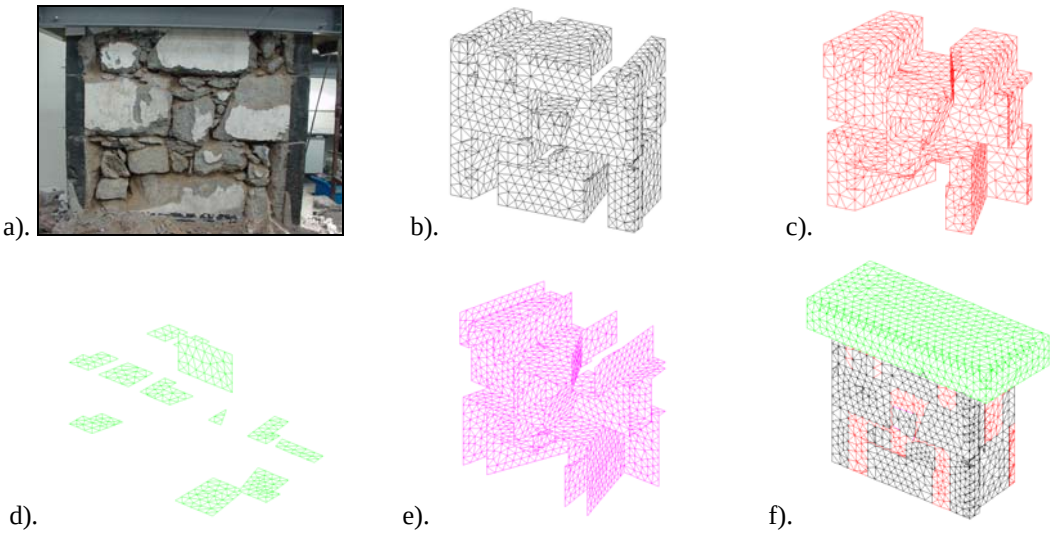

Figure 6: Geometry of the wall: a) real full geometry; b) blocks (FEM); c) infill (FEM); d) joints block-block (FEM); e) joints block-infill; f) final full FEM

Table 1 - Mechanical parameters used in the numerical model

	Elastic modulus E (GPa)	Volumic weight ρ (kN/m^3)
Blocks	28.7	26.0
Infill	0.25	18.0
Joints	Normal stiffness k_n (kPa/mm)	Tangent stiffness k_s (kPa/mm)
Block/block	4.74 x 10^3	6.8 x 10^2
Block/infill	62.41	6.78

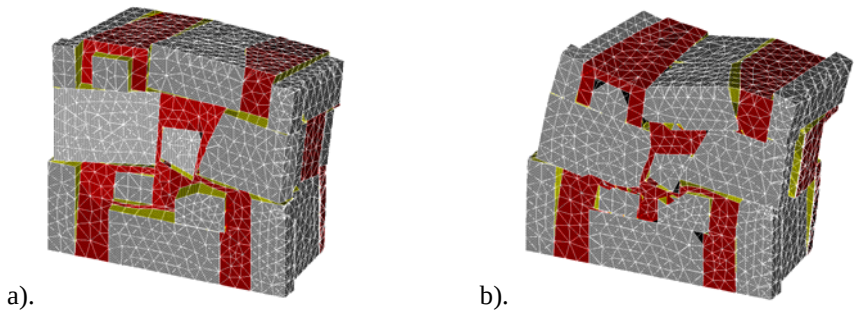

Figure 7: Modes of vibration shapes: (a) 1st mode (transversal); (b) 2nd mode (longitudinal)

Table 2 - Modal analysis comparison

	Experimental (Hz)	Numerical (Hz)
1st mode	19.53	19.68
2nd mode	27.34	27.33

The nonlinear characteristics of joints and infill were defined in order to correctly characterize the behaviour of the tested specimen. Therefore, an elastic-perfectly plastic Drucker-Prager's model with associated yield conditions and without stress hardening, as implemented in CAST3M (Drucker *et al.*, 1952), (Duchesne *et al.*,

1997), was used for the infill taking the values of 10 kPa and 32 kPa, respectively, for f_t (uniaxial tensile strength) and f_c (uniaxial compressive strength).

For the joints nonlinearity, a softening joint model implemented in Cast3m (Pegon *et al.*, 1996) was used, with nonlinear parameters calibrated to match the experimental results starting from those used by (Almeida, 2000) and (Costa, 2002b). The adopted monotonic curves regarding shear behaviour are shown in Figure 8 where trilinear rules are depicted for each joint type (between adjacent blocks and for block/infill interface). Concerning normal stress modelling, zero tensile strength was assumed and linear elastic behaviour is considered for compression.

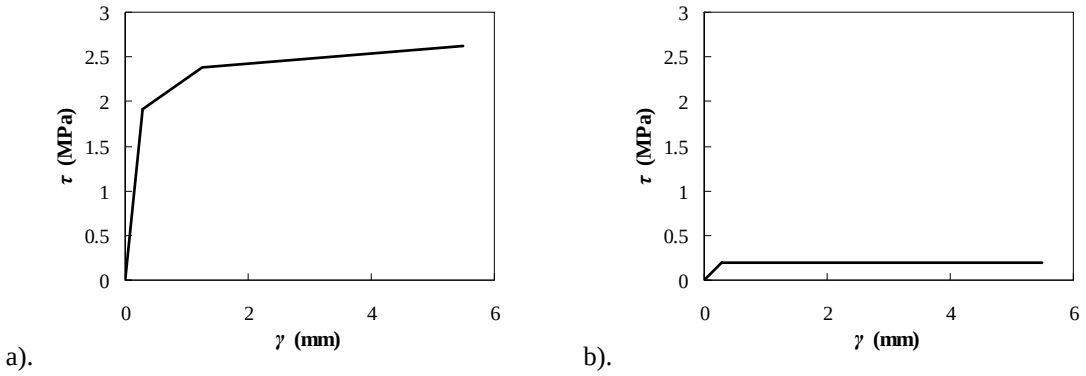

Figure 8: Nonlinear shear behaviour of joint elements: (a) block/block joints; (b) block/infill joints

4.2. Numerical results

The numerical analyses consisted on the full simulation of the experimental test, regarding axial load and displacement levels. The simulation output can be observed in Figure 9 that allows evidencing the numerical model accuracy by comparing the numerical results with the experimental ones. It can be seen that the hysteretic behaviour is globally well described by the model, since it is able to approximately reach the maximum strength (although slightly overestimated), while accounting for the observed stiffness/strength decrease and dissipated energy.

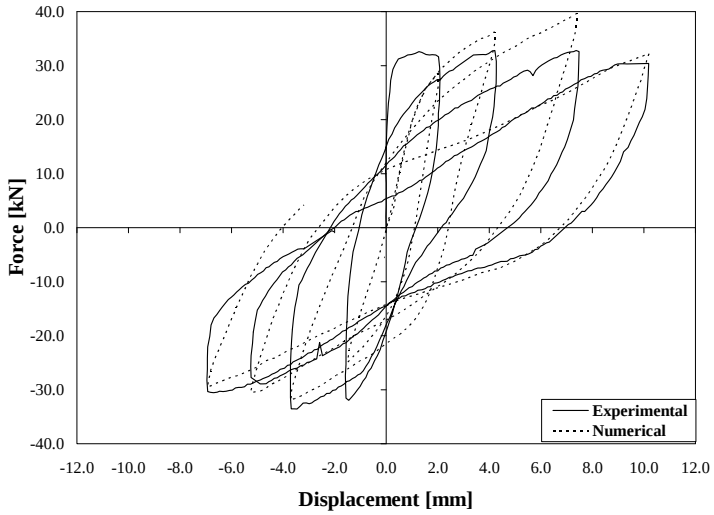

Figure 9: Numerical results vs. experimental results

Beyond this global comparison between numerical and experimental results, the use of this micro-modelling approach allows also comparing numerical and experimental findings concerning lateral displacements along the

height (1/3 and 2/3 of total height) as well as torsional effects exhibited by the tested specimen (monitored in spots 28 and 29 evidenced in Figure 3); these further comparisons are presented in Figure 10. Results show that, at local level, the numerical model is less accurate and only partially reproduced the experimental results in terms of wall displacements (up to the last third of the test).

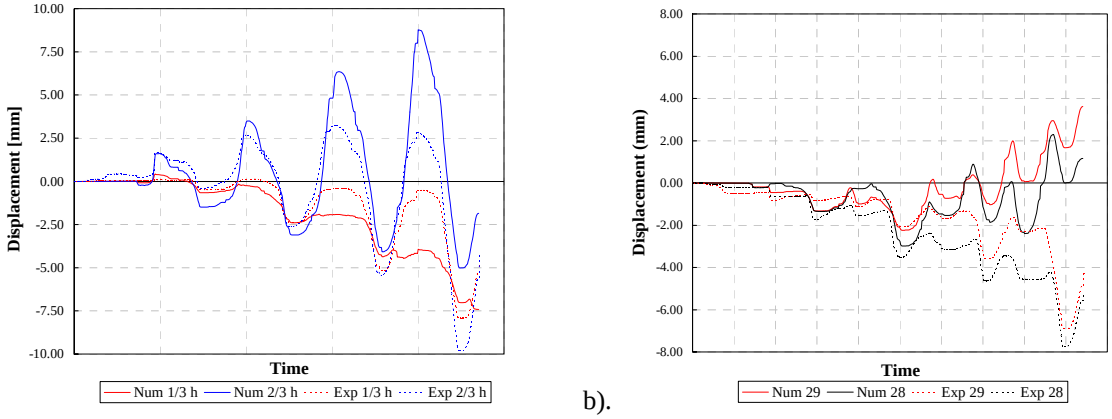

Figure 10: Comparison between numerical and experimental results: a) lateral displacements; b) torsion

5. STRENGTHENING/RETROFIT

The retrofit strategy used in the damaged wall was one of the techniques applied to retrofit/rehabilitate the damaged masonry structures in Faial Island after the earthquake. The adopted scheme modifies the masonry elements into a more confined and homogeneous component behaving monolithically, similar to a reinforced concrete wall with poor concrete.

5.1. Technique description

In this section the technique used to retrofit the wall is briefly presented, always accompanied with explicit figures clarifying each step followed. Hence, Table 3 presents each operation necessary to complete the wall retrofit as well as the time required to perform it; Figure 11 complements the referred table.

Table 3.Working hours vs. operations

	Initial Time	Final Time	Operation
Day 1	8h30m	11h15m	Cover removal
	11h30m	11h40m	Mortar preparation
	11h55m	12h08m	Introduction of the steel rods; Placement of the mortar – 1st phase
	13h20m	15h10m	Placement of the mortar on the West face; Placement of the metallic mesh
	15h25m	15h45m	Installation of the steel plates and tightening of steel rods
	15h50m	16h10m	Introduction of a metallic mesh above the steel plates
Day 2	8h30m	17h	Placement of the mortar – 2nd phase

a). 

b). 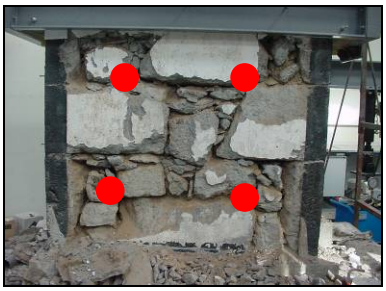

c). 

d). 

e). 

f). 

g). 

h). 

i). 

j). 

Figure 11: Retrofitting technique: a) cover removal; b) position of the steel rods; c) placement of the rods; d) mortar (1st phase); e) installation of the steel mesh; f) placement of the steel plates and tightening; g) installation of the steel mesh above the plates; h) cutting the excess of steel rods; i) mortar cover (2nd phase); j) mortar cure simulating Azores' humidity

5.2. Experimental test

In order to assess the efficiency of the retrofit/strengthening technique, a subsequent experimental test was prepared based on the previous one (unreinforced specimen).

However, this second experimental activity can be considered as a set of three different experimental tests, because, due to the excellent behaviour of the wall with almost no degradation, three different axial load levels were successively applied to the same specimen in three distinct test stages. Thus, starting from 40 kN (original axial load), two other test stagse were accomplished with 100 kN and 160 kN vertical force (respectively, 2.5 and 4 times the basic axial load).

Hence the same initial vertical load was applied to the tested specimen, as well as the same target displacements. However, larger displacements were in fact achieved due to the rocking behaviour of the wall, as described in the next section.

Regarding the monitored points during the experimental test, a slight modification was made (Figure 12) aiming at measuring possible shear distortion (spots 1, 2, 3 and 4 in Figure 12) and some rocking of the foundation (with spots 13 and 14) during the test.

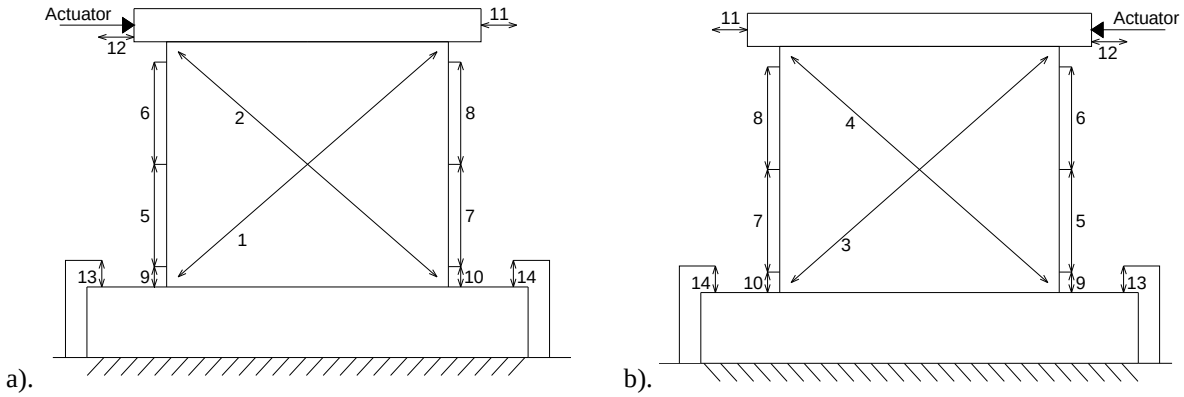

Figure 12: Monitored points on the retrofitted specimen: a) Front view; b) Back view

5.3. Results obtained

Results obtained from the experimental test on the retrofitted masonry pier are presented in Figure 13 for the three different levels of axial load (40 kN, 100 kN and 160 kN). In addition, bilinear idealizations of the response are also included in order to obtain displacement ductility capacity for each axial load level.

Figure 13 allows concluding that the retrofitted specimen behaved monolithically exhibiting pure rocking with low energy dissipation. It should be mentioned, however, that the maximum imposed displacement for the axial load of 100 kN (Figure 13-b) was lower than the other ones because the observed behaviour for this axial load level was similar to the previous test (N = 40 kN) for which a rocking motion governed the response. Indeed, the axial load increase did not change the specimen behaviour and, therefore, the test was stopped and the vertical load was further increased aiming at obtaining a different behaviour mode (by diagonal cracking).

The general trend shows that the maximum displacement obtained for each axial load level did not have strength decrease or larger hysteresis, which is meaningful of complete integrity and material homogeneity.

For the first level of axial load (N = 40 kN), the maximum obtained strength was 42 kN, i.e, 30% larger than the value of 32 kN obtained with the unretrofitted specimen. The maximum achieved drift was 1.1 %, but it was clear that larger displacements could be imposed without any problem. The apparent displacement ductility capacity for this axial load level was 6.5, using a bilinear idealization of the response based on the Eurocode 8 (CEN, 2005); note that, for this rocking behaviour, to similar results would be obtained if the Italian Code proposal (OPCM no. 3274, 2005) or the recent proposal by (Costa, 2007) was used.

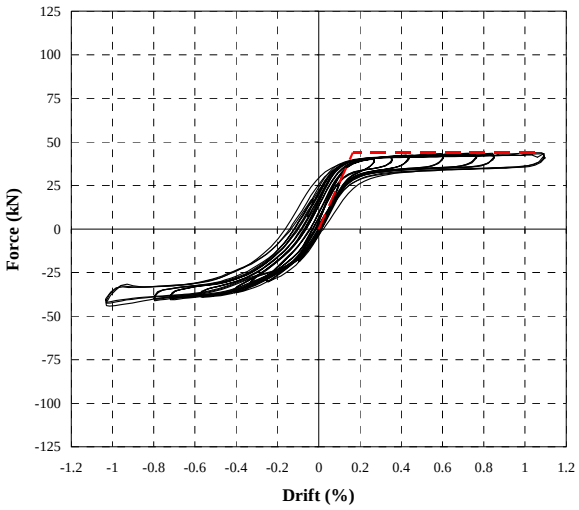

a).

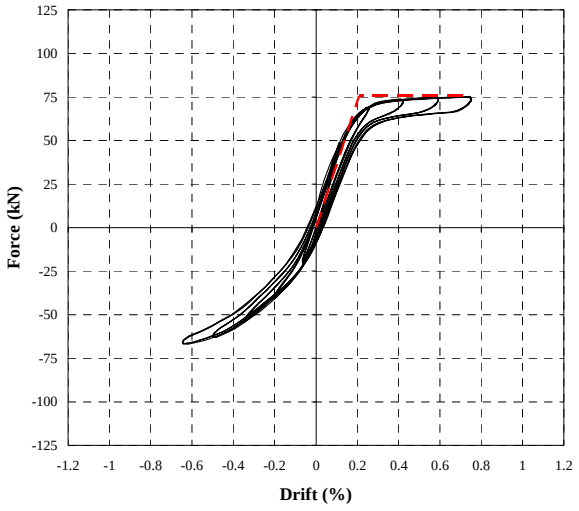

b).

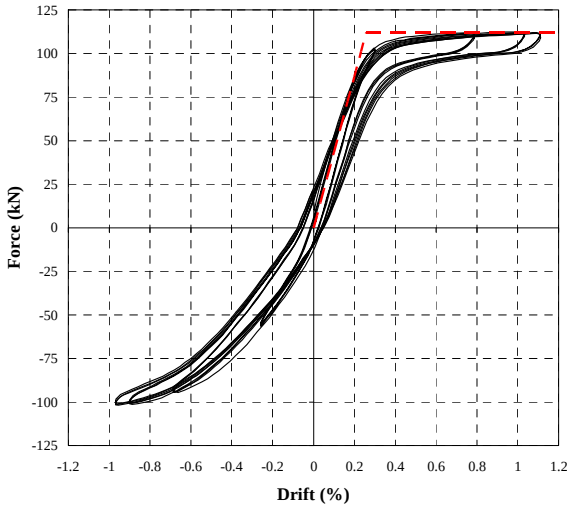

c).

Figure 13: Force vs. displacement curves and bilinear idealization: a) N = 40 kN; b) N = 100 kN; c) N = 160 kN

By increasing the axial load up to 100 kN, a maximum strength of 75 kN was achieved with the same rocking behaviour. However due to the small amount of actually imposed displacement levels, a comparison of the involved displacement ductility is not meaningful.

The higher level of axial load (160 kN) increased the maximum specimen strength up to 112 kN and the available displacement ductility (for the same maximum displacement level) was 4.3, a lower value due to the shifting of the yield point. The energy dissipation capacity remained similar with this axial load level, mainly due to the rocking mechanism.

Figure 14 presents the influence of axial load level on two different results: the maximum strength and the equivalent stiffness. As expected, the axial load influences approximately linearly the maximum strength of the specimen because the "failure" mechanism is not changed. However, if higher levels of axial load were used, a different shape on Figure 14 a) should be obtained due to the change of failure mechanism or due to the maximum resistance envelope related with rocking behaviour. Figure 15 helps on clarifying the axial load influence of on the maximum strength of a hypothetic wall (not the tested specimen) in order to exemplify the expected behaviour. Concerning the equivalent stiffness values (computed using a bilinear idealization as described before) plotted in Figure 14 b), it can be observed a sort of quadratic influence of the axial load on the stiffness values.

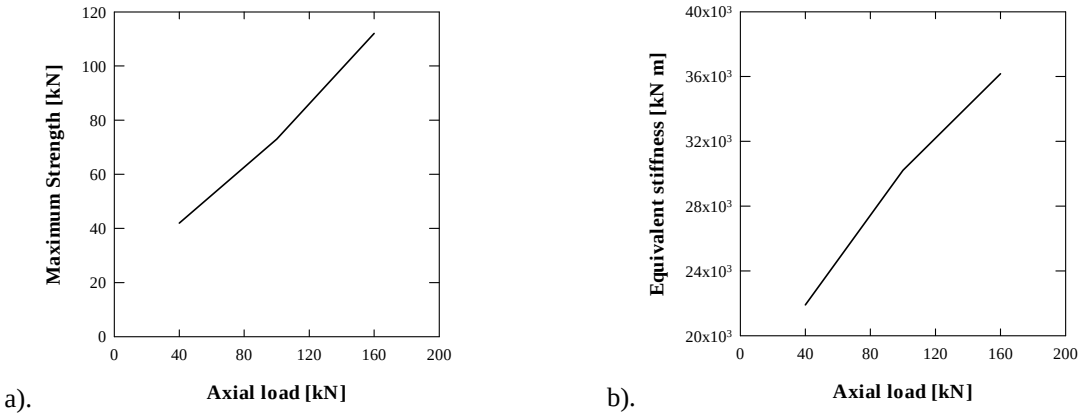

Figure 14: Influence of axial load on: a) maximum strength; b) equivalent stiffness

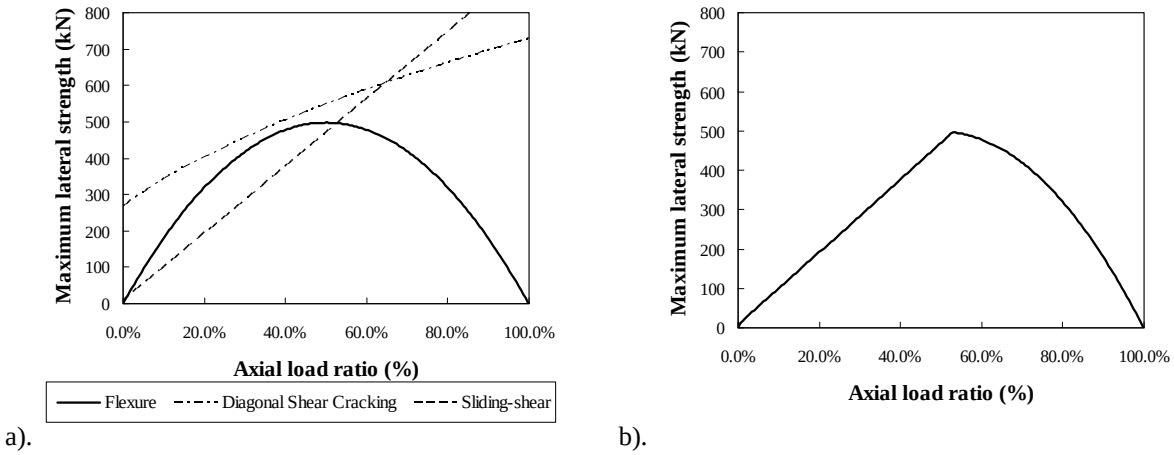

Figure 15: Influence of axial load on maximum strength and failure mode for a hypothetic specimen: a) interaction diagram for each failure mode; b) envelope of the interaction diagram

6. DISCUSSION

The work performed allowed assessing three different topics, namely: in-plane behaviour of the traditional stone constructions; reproducibility using numerical modelling; efficiency of a retrofit/strengthening technique used after the 1998 Azores earthquake.

The in-plane behaviour revealed by the tested specimen was good concerning energy dissipation but achieved through a non-ductile and not controlled behaviour mechanism (shear). Despite being performed only one cycle per displacement level, the strength decrease after peak was significant (80-85%) with a maximum drift level of 0.85 %. Moreover the wall did not keep its integrity during the in-plane loading, which constituted one of the main problems because the strength decrease for the same displacement level was about 20%. Therefore, it is possible to conclude that the wall did not behave satisfactory during the test.

Regarding the numerical modelling, it was possible to verify that, using a micro-modelling approach, the numerical simulation was able to reproduce the tested specimen behaviour, as shown in Figure 9. Despite the complexity of the geometric model, the complete discretization of the wall permitted to assess local displacements, amongst some other information not presented in this work.

Finally, concerning the retrofit efficiency, Figure 16 presents a final comparison between the original wall vs. retrofitted specimen for the same axial load level. As can be observed, the modification of the wall behaviour of the changed completely the energy dissipation of the wall, as also as the integrity and maximum drift attained (retrofitted - 1.15% vs. original - 0.85%). Moreover larger displacements could be easily achieved with the retrofitted specimen as explained previously.

So it is possible to infer that the retrofit/strengthening technique used after the 1998 Azores earthquake is adequate and effective maintaining the integrity of the wall. In addition, since this technique was in-situ used in all the elements and not just on piers or spandrels, a good behaviour of complete structures should be expected with more energy dissipation.

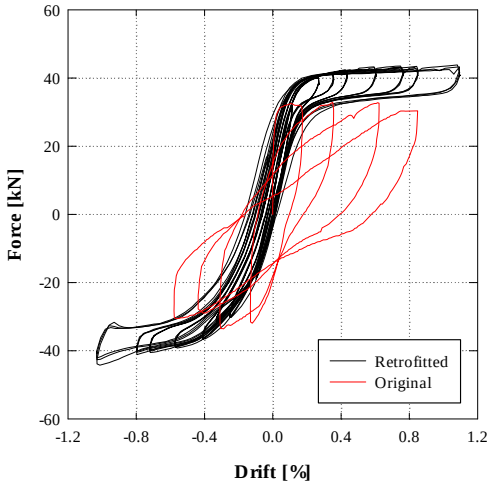

Figure 16: Retrofit efficiency: original vs. retrofitted results

7. CONCLUSIONS

A general overview including different topics was performed on this work, starting with the in-plane behaviour characterization of a stone masonry pier, passing by a complex numerical modelling of the tested specimen, and finally assessing the efficiency of a retrofit/strengthening technique.

The experimental test allowed observing that the behaviour of traditional stone masonry walls is mainly in shear due to poor joint shear strength and to heterogeneity of the materials. However this behaviour may be substantially improved if an adequate strengthening technique is implemented to ensure a homogenous

behaviour given by a correct connection between wall leafs with infill grout to improve the infill and joints behaviour.

Finally the behaviour of a traditional stone masonry wall may be correctly reproduced using a micro-modelling of the complete geometry and by making use of nonlinear models for the joints and infill; this achievement is also very important for a future calibration of simpler models or even to model complete structures.

8. ACKNOWLEDGEMENTS

The authors would like to acknowledge some important persons that helped to perform this work since its first stage, namely Ms. Daniela Glória and Mr. Valdemar Luís from the Laboratory for Earthquake and Structural Engineering (LESE) of the Faculty of Engineering of the University of Porto (FEUP), as also as Ms. Cristina Costa for her help during the development of the numerical model.

9. REFERENCES

Almeida, C. (2000) Análise do Comportamento da Igreja do Mosteiro da Serra do pilar sob a Acção dos Sismos. Porto, Portugal: Faculdade de Engenharia da Universidade do Porto.

CEA (2003) Manuel dútilisation de Cast3m – www.cast3m.cea.fr. Saclay: Commissariat à l'Énergie Atomique.

CEN,(2005) Eurocode 8: Design of Structures for Earthquake Resistance, Part 1: General rules, seismic actions and rules for buildings. Brussels, Belgium: CEN.

Costa, A. (2002a) Determination of Mechanical Properties of Traditional Masonry Walls in Dwellings of Faial Island, Azores. Earthquake Engineering and Structural Dynamics. 37:7. p.

Costa, A. A. (2007) Experimental Testing of Lateral Capacity of Masonry Piers. An Application to Seismic Assessment of AAC Masonry Buildings. Pavia, Italy: European School for Advanced Studies in Reduction of Seismic Risk (ROSE School),.

Costa, C. (2002b) Análise do Comportamento da Ponte da Lagoncinha sob a Acção do Tráfego Rodoviário. Porto, Portugal: Faculdade de Engenharia da Universidade do Porto.

Drucker, D. C.; Prager, W. (1952) Soil Mechanics and Plastic Analysis or Limit Design. Quarterly of Applied Mathematics. 10: p. 157-165.

Duchesne, A.; Raepsaet, X. (1997) Un Modèle Élasto-Plastique de CASTEM 2000 Utilisable pour la Modélisation du Comportement Mécanique d'Un Lit de Particules. Ispra: CEA.

INE (2002) Censos 2001. Lisboa.

OPCM no. 3274 (2005) Primi elementi in materiali di criteri generali per la classificazione sismica del territorio nazionale e di normative tecniche per le costruzioni in zona sísmica, come modificato dall'OPCM 3431 del 3/5/05 (in Italian).

Pegon, P.; Pinto, A. V. (1996) Seismic Study of Monumental Structures – Structural Analysis, Modelling and Definition of Experimental Model. Ispra: JRC.